International Journal of Thermophysics, Vol. 24, No. 3, May 2003 (© 2003)

Measurement of Thermal Transport Properties with an Improved Transient Plane Source Technique[1]

M. Anis-ur-Rehman[2] and A. Maqsood[2, 3]

The transient plane source (TPS) technique has been revised with the aim of developing a simple and fast system to measure the thermal transport properties of materials at low temperatures, especially high-T_c superconductors. To ensure reliable results, any new system should be tested with known samples. Fused silica, 0.9% carbon steel (215/3), and halide crystals (silver chloride) were studied with the new setup to check its performance. Data were taken from room temperature down to liquid nitrogen temperature. The assembly was designed for cryogenic (79 to 300 K) measurements in an atmosphere free of humidity. Dry nitrogen gas was used as a heat transfer medium around the sample holder assembly. The measured values for thermal conductivity and thermal diffusivity of these samples are in excellent agreement with values reported earlier. The thermal conductivity and thermal diffusivity for silver chloride crystals are extended down to 80 K although recommended data were available only down to 220 K. A Ba-doped, Bi-based, high-T_c superconductor was prepared by a solid-state reaction method. The nominal composition used was $Bi_{1.6}Pb_{0.4}Sr_{1.6}Ba_{0.4}Ca_2Cu_3O_y$. Large-sized samples (diameter $\sim$ 28 mm and length $\sim$ 11 mm) are investigated for thermal transport properties.

KEY WORDS: bismuth-based superconductor; carbon steel; fused silica; hot-disk sensor; thermal conductivity; thermal diffusivity; transient plane source method; Wheatstone bridge.

1. INTRODUCTION

The exciting superconducting mechanism has attracted physicists to investigate the properties of new high-T_c superconductors, not only experimentally

[1] Paper presented at the Sixteenth European Conference on Thermophysical Properties, September 1–4, 2002, London, United Kingdom.

[2] Thermal Physics Laboratory, Department of Physics, Quaid-i-Azam University, Islamabad 45320, Pakistan.

[3] To whom correspondence should be addressed. E-mail: tpl@qau.edu.pk and tpl.qau@usa.net

0195-928X/03/0500-0867/0 © 2003 Plenum Publishing Corporation

but also theoretically. Thermal conductivity is one of the most useful probes to investigate the interaction between electronic (λ_e) and phonon thermal conductivity (λ_{ph}).

One of the classes of methods for the measurement of thermal transport properties is formed by the transient methods. These methods assume that initially the specimen is at thermal equilibrium with the surrounding atmosphere. Then a stepwise electric current is fed to the sensor. The sensor is embedded within two specimens. During the time of measurement the change in temperature of the sensor is monitored. By correlating the experimental temperature measurements with the theoretical formulation, e.g., [1] the thermal diffusivity is evaluated. One of the transient techniques is the transient plane source (TPS) technique [2, 3], which is one of the methods of the contact temperature-time measurement family. This technique can be used over a broad range of temperatures, i.e., from 77 to 1073 K [4, 5]. Thermal conductivity measurements can be carried out within the range of 0.005 to 500 $W \cdot m^{-1} \cdot K^{-1}$ [6]. The TPS technique is an extension of the transient hot-strip (THS) method [7] that is based on the strip heat source method. With the TPS method, for a known rate of heat flow the temperature changes in time are monitored as a measure of the thermal transport properties. Then simultaneous determination of thermal conductivity and thermal diffusivity is also possible.

Emphasis is placed on the apparatus, the instrumentation, and the computerized data acquisition design as well as on the demonstration as a purposeful and characteristic example of application. A description of the mechanical design and the test results for the high-T_c superconducting sample are also presented. The designed system accomplishes the following objective: acquisition of data with high speed and high accuracy. Specimen size variation is also incorporated by using TPS sensors of different sizes.

2. THEORETICAL BACKGROUND

The TPS method considers the three-dimensional heat flow inside the specimen. The specimen is regarded as an infinite medium. The technique uses a "resistive element" (the TPS element) both as a heat source and temperature sensor. The time-dependent temperature increase $\Delta T(t)$ gives rise to a change in the electrical resistance, $R(t)$, of the conducting pattern shown in Fig. 1, and may be expressed as [8]

$$R(t) = R_0(1 + \alpha \overline{\Delta T(t)}) \tag{1}$$

Here R_0 is the resistance of the TPS element before transient recording has been initiated, α is the temperature coefficient of resistivity (TCR), and

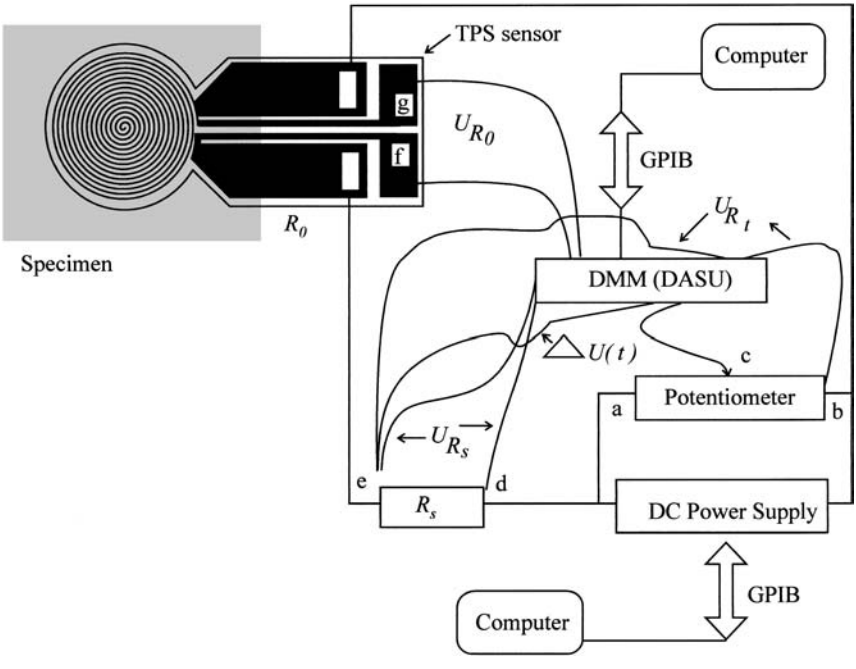

Fig. 1. Principal electrical circuit for the modified bridge arrangement, showing TPS sensor (R_0) with specimen, standard resistance (R_s), potentiometer, dc power supply, DASU, and points of measuring voltages.

$\overline{\Delta T(t)}$ is the mean value of the time-dependent temperature increase of the TPS element. For convenience and as an experimental requirement, to obtain the thermal conductivity and thermal diffusivity simultaneously, the mean temperature change of the sensor is defined in terms of the dimensionless variable τ, where

$$\tau = \left(\frac{t}{\theta}\right)^{\frac{1}{2}} \tag{2}$$

and

$$\theta = \frac{r^2}{a} \tag{3}$$

where t is the time measured from the start of transient heating, a is the thermal diffusivity of the specimen, θ is the characteristic time, and r is a constant that represents a measure of the overall size of the resistive pattern

(= radius of hot disk). During the transient event, $\overline{\Delta T(\tau)}$ can be considered as a function of time only, whereas, in general terms, it will depend on such parameters as the output power in the TPS element, the design function ($D_s(\tau)$) of the resistive pattern, and the thermal conductivity, λ, and thermal diffusivity, a, of the surrounding material. Using the ring-source solution [1], it is possible to write down an exact solution for the bifilar spiral or hot disk as follows:

$$\overline{\Delta T(\tau)} = \frac{P_0}{R\lambda\pi^{3/2}} D_s(\tau) \tag{4}$$

Here P_0 is the total power output, and $D_s(\tau)$ is the design function of the resistive pattern defined elsewhere [2].

If all heat is transported via a solid specimen, the thermal conductivity, λ, the thermal diffusivity, a, and the heat capacity per unit volume, ρC_p, are expressed by

$$a = \frac{\lambda}{\rho C_p} \tag{5}$$

When calculating the average temperature according to Eq. (4), it must be remembered [3] that the concentric ring sources have different radii and are placed at different temperatures for the transient recording. This becomes very obvious when remembering that $\overline{\Delta T(\tau)}$ is intended to describe the total resistance change. The temperature increase during the transient measurement is kept within 1 K [9] so Eq. (5) is applicable in our case.

Starting from the above theory, the thermal transport properties can be determined using an appropriate curve-fitting technique for the measured temperature versus time points. A detailed description of this experimental technique can be found elsewhere [2]. The ideal model presupposes that the double spiral sensor, assumed to consist of a set of equally spaced, concentric, and circular heat sources, is sandwiched in specimens of infinite dimensions. In practice, all real specimens have finite dimensions. However, by restricting the time of the transient which is related to the thermal penetration depth of the transient heating, a measurement can still be analyzed as if it were performed in an infinite medium. This means that the ideal theoretical model is still valid within a properly selected time window for the evaluation. Also the sensitivity coefficients [10, 11] are the theoretical foundation for determining a suitable time window to be used in the curve-fitting procedure.

To record the potential difference variations that correspond to the temperature change during the transient recording period, a modified bridge arrangement was used as shown in Fig. 1. The circuit components are reduced with this new arrangement as compared to the bridge used earlier [5]. The thermal conductivity of superconducting materials is temperature dependent, and to see this effect, an arrangement is required for changing the temperature of the material with time. With this aim a simple cryostat was designed comprising (a) a liquid nitrogen Dewar, (b) one end closed hollow stainless steel cylinder with a vacuum valve, (c) rotary vacuum pump, (d) dry nitrogen gas cylinder with filler arrangement, and (e) a sample holder assembly as shown in Fig. 2. This cryostat could be used to vary and maintain the required temperature from room temperature down to the boiling point of liquid nitrogen. The specimen holder used with the new bridge arrangement is also shown in Fig. 2. The specimen pieces are clamped together firmly with the help of a steel strip and screw arrangement. The screws are used to provide further tightening, if required, to adjust the position of the specimens under investigation. The bridge is in the balanced mode shortly before the transient recording period. During the transient run the bridge is somewhat out of balance. If we assume that the resistance increase will cause a potential difference $\Delta U(t)$ measured by

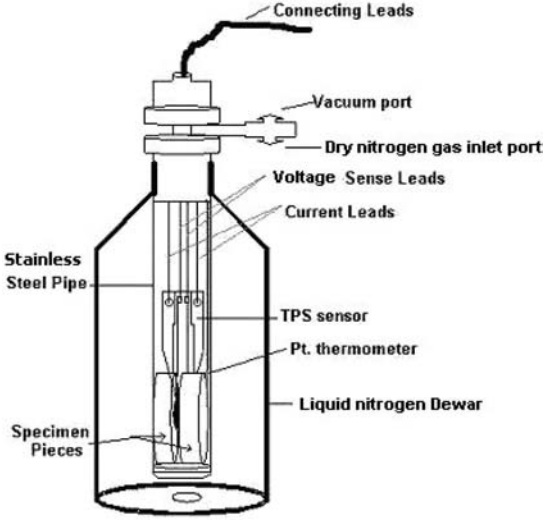

Fig. 2. Specimen holder assembly showing the TPS sensor sandwiched between two test specimen pieces and the surrounding temperature measurement and control arrangement.

the voltmeter (DMM) in the bridge, the analysis of the bridge indicates that the temperature will vary as described below

$$\overline{\Delta T(t)} = \frac{\Delta U(t)}{1.0 - \Delta U(t)/R_s i_0} \frac{(R_t + R_s)}{(\alpha R_0 R_s i_0)}, \tag{6}$$

where R_s is the high power standard resistor, and R_t, between points b and e (Fig. 1), is the total resistance of the TPS sensor (R_0) and connecting leads (R_L) before the transient run and is given by

$$R_t = \frac{R_s U_{R_t}}{U_{R_s}} \tag{7}$$

Here, U_{R_t} is the voltage across the resistor R_t and between the points b and e; ($R_t = R_0 + R_L$); U_{R_s} is the voltage across the standard resistor R_s; and i_0 is the heating current through the sensor during the transient run.

It is to be noted that the resistance of the TPS sensor is calculated from the same experiment and that no separate experiment is required which can be expressed as

$$R_0 = \frac{R_s U_{R_0}}{U_{R_s}} \tag{8}$$

U_{R_0} is the voltage across the TPS sensor.

The accuracy of the resistance measurement of the TPS sensor plays an important role in the calculation of thermal parameters, so an exact value up to 10 μΩ is achieved by the above procedure.

3. EXPERIMENTAL ARRANGEMENT

The bridge circuit used is shown in Fig. 1. The electrical circuit consists of an HP 6633B dc power supply, R_s-standard resistance, potentiometer, and digital data acquisition switch unit (DASU) Agilent 34970A with internal DMM and TPS element R_0. DASU is used to measure quasi-simultaneous voltages at the points d and e (U_{R_s}), f and g (U_{R_0}), and b and e (U_{R_t}) of the circuit before and after the transient run. Also, the voltage variations ($\Delta U(t)$) (200 measurement points) across the bridge circuit during the transient run are measured by DASU. The dc output power of the power supply unit that is used for balancing the bridge and heating the TPS element, is controlled through the computer. For balancing the bridge, a very low current is supplied to the circuit so that it works for balancing

but does not actually heat the TPS sensor. The choice of balancing current and transient heating current depends upon the experimental conditions and specimen under investigation. The constant current during transient heating should be chosen such that the total temperature increase does not exceed 1 K.

A hot disk sensor is, in principle, a very sensitive (resolution better than millikelvin) resistance thermometer, which is used for recording the temperature excursion during a transient run. The collected data are vulnerable to distortion if there is any temperature drift in the specimen or in the whole experimental assembly, resulting in erroneous calculations of the thermal parameters. This could be compensated either by measuring the temperature drift or allowing the system to relax.

3.1. Temperature Drift Measurement

In certain cases it is difficult to achieve a homogeneous temperature distribution around the specimen assembly (the sensor and specimen pieces), particularly when cooling to liquid nitrogen temperature. This could be compensated by monitoring the temperature variation, $\Delta T_d(t)$, of the element, owing to the temperature drift. Immediately after the temperature drift measurement, the transient experiment is performed. The value of the actual change in temperature $\Delta T_a(t)$ is obtained by subtraction of $\Delta T_d(t)$ from the measured $\Delta T(t)$ value, i.e.,

$$\Delta T_a(t) = \Delta T(t) - \Delta_d(t)$$

The minimum time used for temperature drift data (100 measurement points) was 25 s and for higher transient measurement times, the drift was measured for half the transient run.

3.2. Time of Relaxation

Initially, the specimen is considered to be of homogeneous temperature and placed in a perfect thermostat so that any temperature variation from the surroundings would not distort the data. The time gap between two consecutive transient experiments, for reliable results, is termed as the time of relaxation and is at least b^2/a, where $b = r$ (radius of specimen) or $b = h$ (height of specimen), whichever value is the greater. a is the thermal diffusivity of the material under study, and it is assumed that the probing depth is equal to the sensor radius. The variation of the sensor radius does not make any difference. With the modified circuit arrangement the relaxation time is reduced by a factor of six.

3.3. Lead Resistance R_L

For the low temperature measurements inside a cryostat [4, 8] or for the high temperature measurements inside a furnace [2, 5], special attention must be paid to eliminating any heating effect of the long leads used. Instead of measuring the resistance R_0 directly by the four-probe method [4], voltages at points b–e and f–g as shown in Fig. 1 are measured to determine

$$U_{R_t} = U_{R_0} + U_{R_L}$$

Using i_0 and Ohm's law, R_L is determined as $R_L = R_t - R_0$.

4. RESULTS AND DISCUSSION

With the purpose of demonstrating that the TPS technique using the modified setup could be used down to the temperature of liquid nitrogen, measurements on fused silica, carbon steel, and silver chloride crystals were performed. The main aim of the whole study is to develop a simple system providing higher accuracy that can be used for the measurement of the thermal transport properties of high-T_c superconductors. After verifying the performance of the setup, the superconducting samples with nominal composition $Bi_{1.6}Pb_{0.4}Sr_{1.6}Ba_{0.4}Ca_2Cu_3O_Y$ were studied. The dimensions of the four types of specimens and radii of the TPS sensor used are given in Table I.

The choice of fused silica is due to the fact that it is an insulator and that its thermal conductivity is well established at low temperatures. Carbon steel is a conductor, and silver chloride is a crystalline material,

Table I. Dimensions of Test Specimens, along with Sensor Radii, Probing Depth, and τ_{max}

S. No.	Test specimen	Diameter (±0.05) mm	Length (±0.05) mm	Sensor radius (±0.001) mm	Probing depth (±0.001) mm	τ_{max}
1	Fused Silica	(a) 35.05 (b) 35.00	(a) 20.30 (b) 20.35	(i) 9.734 (sensor 1) (ii) 3.300 (sensor 2)	(i) 8.645 (ii) 6.500	(i) 0.50 (ii) 0.98
2	Carbon Steel (SS215/3)	(a) 38.15 (b) 38.25	(a) 19.70 (b) 19.50	9.734	15.260	0.78
3	Silver Chloride crystals	(a) 25.40 (b) 25.40	(a) 4.30 (b) 4.25	3.300	3.972	0.60
4	$Bi_{1.6}Pb_{0.4}Sr_{1.6}Ba_{0.4}Ca_2Cu_3O_y$ superconductor	(a) 28.01 (b) 28.02	(a) 11.12 (b) 11.31	3.300	7.473	0.41

thus measurements on these materials will help to determine the reliability of the technique for conductors and crystalline materials. The measurements are carried out as a function of temperature for all three specimens. Due to the availability of data for the thermal conductivities of the studied specimens from other sources (with different techniques), comparisons of thermal conductivities are made.

4.1. Fused Silica

Data for the silica specimens were taken with sensors having radii of 9.734 ± 0.001 mm (sensor 1) and 3.300 ± 0.001 mm (sensor 2). The variation of the thermal conductivity with temperature is shown in Fig. 3, and the results are tabulated in Table II. The results obtained are compared with the recommended experimental values [12] and also with the previously calibrated bridge circuit [8]. The differences do not exceed 1% at any temperature. Previously reported differences were 1% at room temperature and 4% at low temperatures [8]. These results show that the performance of TPS has been improved.

The measurement times used were 10 to 20 s for sensor 1 and 10 s for sensor 2. The currents used for balancing were in the range of 1.5 to 3 mA

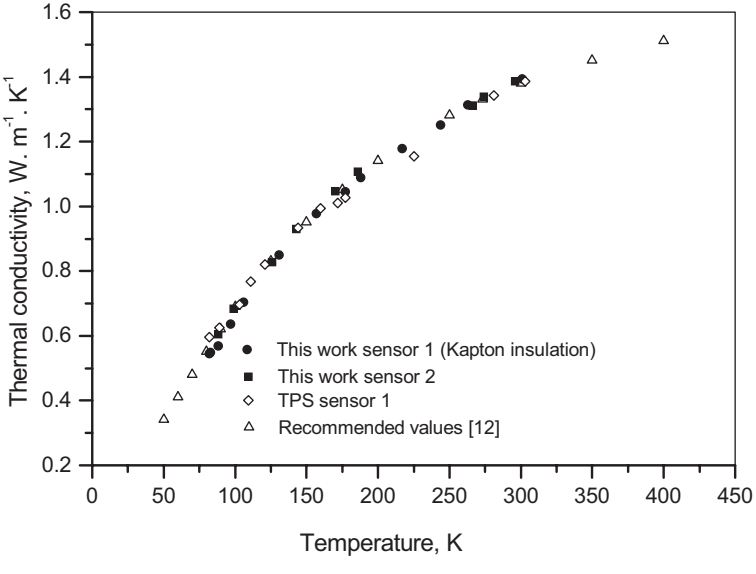

Fig. 3. Variation of the thermal conductivity of fused silica samples with temperature.

Table II. Thermal Conductivities (in $W \cdot m^{-1} \cdot K^{-1}$) of Fused Silica from Other Sources and from Both Sensors Used in the Present Work

S. No.	T (K)	(i)[a]	(ii)[b]	Sensor 1	Sensor 2
1	50	0.34±0.03	–	–	–
2	60	0.41±0.03	–	–	–
3	70	0.48±0.03	–	–	–
4	80	0.55±0.03	–	–	–
5	82	–	0.595±0.020	0.5542±0.0007	–
6	88	–	–	0.6041±0.0008	0.6061±0.0008
7	89	–	0.625±0.021	–	–
8	90	0.62±0.04	–	–	–
9	97	–	–	0.6744±0.0009	–
10	100	0.69±0.03	–	–	0.6840±0.0009
11	103	–	0.696±0.023	–	–
12	106	–	–	0.7048±0.0010	–
13	111	–	0.768±0.024	–	–
14	121	–	0.821±0.024	–	–
15	125	0.83±0.03	–	–	0.8287±0.0011
16	131	–	–	0.8501±0.0011	–
17	144	–	0.933±0.027	–	0.9306±0.0013
18	150	0.95±0.03	–	–	–
19	157	–	–	0.9782±0.0013	–
20	160	–	0.995±0.028	–	–
21	172	–	1.010±0.028	–	1.0471±0.0014
22	175	1.05±0.04	–	–	–
23	177	–	1.026±0.025	1.0465±0.0014	–
24	188	–	–	1.0899±0.0015	1.1077±0.0015
25	200	1.14±0.04	–	–	–
26	204	–	–	–	1.1186±0.0015
27	217	–	–	1.1791±0.0016	–
28	225	–	1.155±0.023	–	–
29	244	–	–	1.2517±0.0017	–
30	250	1.28±0.04	–	–	–
31	263	–	–	1.3144±0.0018	–
32	266	–	–	–	1.3127±0.0018
33	273	1.33±0.04	–	–	1.3391±0.0018
34	281	–	1.342±0.026	–	–
35	296	–	–	–	1.3873±0.0019
36	300	1.38±0.04	–	–	–
37	301	–	–	1.3940±0.0019	–
38	303	–	1.386±0.027	–	–
39	350	1.45±0.04	–	–	–
40	400	1.51±0.04	–	–	–

[a] Touloukian and Powell, 1970 [12].
[b] Calibrated bridge by Maqsood et al., 1996 [8].

and for measurements, the current values ranged from 149 to 325 mA. Balancing currents and measurement currents decrease as the temperature is increased as the resistance of the TPS sensor and the connecting leads changes with temperature.

4.2. Carbon Steel

Carbon steel specimens, SS215/3, obtained from Analytical Standards AB Sweden, were analyzed from room temperature down to the boiling point of liquid nitrogen. A plot of the thermal conductivity variation with temperature and composition of the specimen is shown in Fig. 4, and the results are tabulated in Table III. A similar trend has been observed in an earlier study [13] for an almost similar composition. They made measurements from room temperature to 573 K. The values for thermal conductivity are in agreement with this report for the same temperature range. Detailed comparisons are made with the data from an earlier measurement [8]. The thermal conductivity values decrease at low temperatures due to the reduction of the electronic contribution to conduction.

4.3. Silver Chloride Crystal

Silver chloride crystals are a useful material for deep IR applications where sensitivity to humidity is a problem. A major use is in the manufacture of small disposable cell windows for spectroscopy, known as a "minicell." The structure of these crystals is cubic, fcc.

These specimens were obtained from Crystran, United Kingdom. Since the measurement period should not significantly differ from the characteristic time (θ) of the measurement, the sensor radius must be determined with care. The heat capacity of the sensor compared to that of the test specimen and the thermal diffusivity of the specimen may also restrict the choice of the sensor size [6]. For the AgCl crystals, only sensor 2 was suitable. Figure 5 shows the variation of thermal conductivity with temperature for the silver chloride crystals, and the results are tabulated in Table IV. A very good match is observed for the available recommended data [12], and also the thermal conductivity values are extended down to liquid nitrogen temperature. These data will be helpful for application to optical windows used at low temperatures. The thermal conductivity values of AgCl are proportional to T^{-1} in the temperature region of the measurement. The detailed calculations will be published elsewhere.

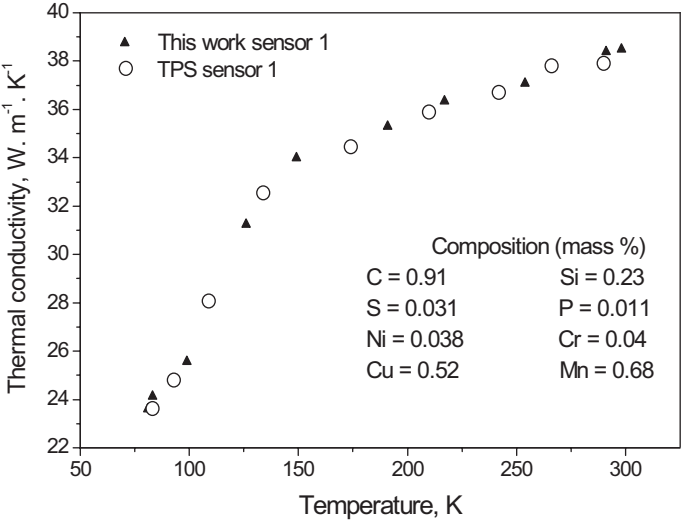

Fig. 4. Variation of the thermal conductivity with temperature for the stainless steel No. 215/3 0.9% carbon.

Table III. Thermal Conductivity (in $W \cdot m^{-1} \cdot K^{-1}$) of Stainless Steel from Circuit Used Previously [8] and the Present Work

S. No.	T (K)	TPS [8]	This work
1	81	–	23.595 ± 0.033
2	83	23.62 ± 0.81	24.120 ± 0.034
3	93	24.81 ± 0.74	–
4	99	–	25.553 ± 0.036
5	109	28.08 ± 0.78	–
6	126	–	31.248 ± 0.044
7	134	32.55 ± 0.80	–
8	149	–	33.973 ± 0.047
9	174	34.45 ± 0.81	–
10	191	–	35.292 ± 0.049
11	210	35.88 ± 0.72	–
12	217	–	36.327 ± 0.051
13	242	36.70 ± 0.73	–
14	254	–	37.068 ± 0.052
15	266	37.79 ± 0.75	–
16	290	37.91 ± 0.75	–
17	298	–	38.495 ± 0.054

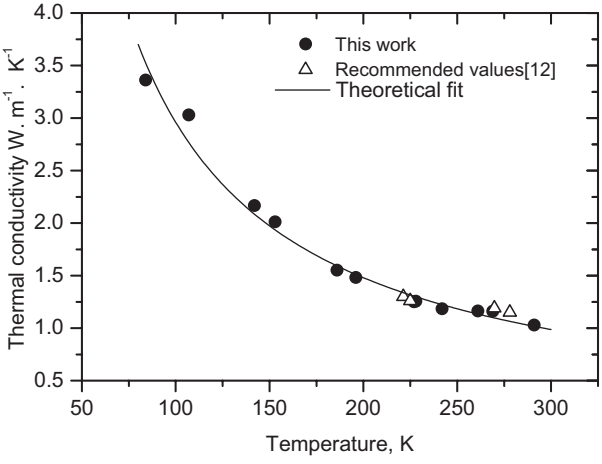

Fig. 5. Variation of the thermal conductivity with temperature for AgCl crystals. Solid line is $\lambda = cT^{-1}$ fit, where c is a constant.

Table IV. Thermal Conductivity (in $W \cdot m^{-1} \cdot K^{-1}$) of Silver Chloride Crystals from Other Sources and the Present Work

S. No.	T (± 1 K)	Other sources [12]	This work
1	84	–	3.3612 ± 0.0047
2	107	–	3.0305 ± 0.0042
3	142	–	2.1661 ± 0.0030
4	153	–	2.0121 ± 0.0028
5	186	–	1.5514 ± 0.0022
6	196	–	1.4823 ± 0.0021
7	221	1.30	–
8	225	1.26	–
9	227	–	1.2511 ± 0.0018
10	228	–	1.2560 ± 0.0018
11	242	–	1.1842 ± 0.0017
12	261	–	1.1643 ± 0.0016
13	269	1.19	1.1612 ± 0.0017
14	278	1.15[a]	–
15	291	–	1.0305 ± 0.0014
16	325	1.09	–

[a] Crystran, United Kingdom.

4.4. Superconducting Samples

A Ba-doped, Bi-based, high-T_c superconductor was prepared by a solid state reaction method. The nominal composition used was $Bi_{1.6}Pb_{0.4}Sr_{1.6}Ba_{0.4}Ca_2Cu_3O_y$. Large-sized samples (diameter ~ 28 mm and length ~ 11 mm) are investigated for thermal transport properties. The size of the samples used for the thermal conductivity measurements was indeed the largest reported for this kind of measurement. Our thermal conductivity results are plotted in Fig. 6 and are tabulated in Table V. The sample shows the same general trend and at $T > T_c$ the thermal conductivity is slightly decreasing, but at $T < T_c$, λ is enhanced.

Because the compound is metallic above T_c, heat can be conducted by both phonons (λ_{ph}) and electrons (λ_e). Thus, the largest contributions to the total thermal conductivity λ above T_c is due to lattice conduction. The sharp up-turn of the measured thermal conductivity and the further increase for $T < T_c$ has three different hypotheses: (i) only the phonons are contributing to this increase (phonon approach); (ii) only the electron contribution is responsible (electron approach); and (iii) both phonon and electron contributions are causing the increase (electron + phonon approach). The electron approach describes the thermal conductivity of a YBCO sample fairly well but seems unsatisfactory in the case of the thermal transport in Bi2223 samples. The phonon approach provides a better estimate of the energy gap with a lower number of free parameters but the best fit is obtained with the electron + phonon approach [14]. Thus the thermal conductivity arises from the decrease in scattering of phonons by carriers as they later condense into superconducting pairs. This will cause a faster increase of λ_{ph}, which predominates the decrease in λ_e leading to a net increase in the measured thermal conductivity. It should be noted that the uncertainties in thermal conductivity values of our data are within 1%. Comparing the results between different laboratories, one notes that the thermal conductivity depends on a particular sample preparation process, while the temperature dependence of the conductivity is similar for all samples [15]. So the order of magnitude of the thermal conductivity (measured by the non-steady-state method in our case) is comparable to the results obtained by different authors [16] (measured by steady-state methods).

5. SUMMARY AND CONCLUSIONS

An improved bridge for the transient plane source has been validated with measurements on fused silica, carbon steel, and silver chloride specimens. At any temperature, the deviation in the evaluated results of the

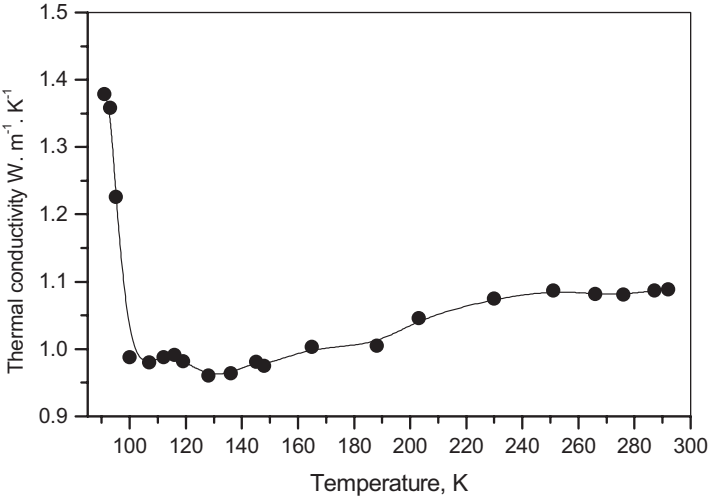

Fig. 6. Variation of the thermal conductivity with temperature for the superconducting samples.

Table V. Thermal Conductivity (in $W \cdot m^{-1} \cdot K^{-1}$) of the Superconducting Samples

S. No.	T (± 1 K)	Thermal conductivity
1	91	1.3791 ± 0.0013
2	93	1.3582 ± 0.0013
3	95	1.2263 ± 0.0017
4	100	0.9883 ± 0.0014
5	107	0.9802 ± 0.0014
6	112	0.9879 ± 0.0014
7	116	0.9917 ± 0.0014
8	119	0.9821 ± 0.0013
9	128	0.9602 ± 0.0013
10	136	0.9638 ± 0.0013
11	145	0.9808 ± 0.0014
12	148	0.9753 ± 0.0014
13	165	1.0032 ± 0.0014
14	188	1.0051 ± 0.0014
15	203	1.0463 ± 0.0015
16	230	1.0752 ± 0.0015
17	251	1.0871 ± 0.0015
18	266	1.0820 ± 0.0015
20	276	1.0811 ± 0.0015

thermal conductivity is less than 2% when compared with recommended values. With the present arrangement, the bridge circuit components are reduced, the temperature drift of the specimens is very well compensated, and the time of relaxation (time between two reliable readings) is minimized. No separate experiment is required to determine the resistance of the TPS sensor at different temperatures, which is calculated very accurately during the same experiment. Instead of measuring the resistance of the TPS sensor directly by the four-probe method (as was done in the circuit arrangement used earlier), the voltages at certain points are measured to determine the sensor resistance, and this makes the new arrangement more precise. The overall goal of being able to enter minimum parameters so there would be no need to make any manual calculations before or during an experiment is also achieved. The thermal conductivity values for sensor 2 are in excellent agreement with those of sensor 1. Thermal conductivity data of Ba-doped high-T_c superconductor as a function of temperature are also reported. The detailed analysis will be published elsewhere.

ACKNOWLEDGMENTS

We wish to thank Silas E. Gustafsson and Mattias K. Gustavsson (Department of Physics and Department of Thermo and Fluid Dynamics, Chalmers University of Technology, Gothenburg, Sweden, respectively) for their useful suggestions during their visit to the Thermal Physics Laboratory and for providing some of the components used in this project. We also owe thanks to M. Maqsood (SSO, KRL, Pakistan) for his cooperation. Also, the authors would like to thank the Pakistan Atomic Energy Commission (PAEC), University Research Fund (Quaid-i-Azam University, Pakistan) and The Abdus Salam International Center for Theoretical Physics (ICTP), Italy, for financially supporting this project.

REFERENCES

1. H. S. Carslaw and J. C. Jaeger, *Conduction of Heat in Solids* (Oxford University Press, Oxford, 1959).
2. S. E. Gustafsson, *Rev. Sci. Instrum.* **62**:797(1991).
3. S. E. Gustafsson, B. Suleiman, N. S. Saxena, and I. Haq, *High Temp.–High Press.* **23**:289(1991).
4. B. M. Suleiman, E. Karawacki, and S. E. Gustafsson, *High Temp.–High Press.* **25**:205(1993).
5. A. Maqsood, M. A. Rehman, V. Gumen, and A. Haq, *J. Phys. D: Appl. Phys.* **33**: 2057(2000).
6. M. Gustavsson, J. S. Gustavsson, S. E. Gustafsson, and L. Halldahl, *High Temp.–High Press.* **32**:47(2000).

7. S. E. Gustafsson, E. Karawacki, and M. N. Khan, *J. Phy. D: Appl. Phys.* **12**:1411(1979).
8. M. Maqsood, M. Arshad, M. Zafarullah, and A. Maqsood, *J. Supercond. Sci. Technol.* **9**:321(1996).
9. S. E. Gustafsson, E. Karawacki, A. J. Hamdani, K. Ahmed, and A. Maqsood, *J. Appl. Phys.* **53**:6047(1982).
10. J. V. Beck and K. J. Arnold, *Parameter Estimation in Engineering and Science* (Wiley, New York, 1977).
11. V. Bohac, M. K. Gustavsson, L. Kubicar, and S. E. Gustafsson, *Rev. Sci. Instrum.* **71**:2452(2000).
12. Y. S. Touloukian and R. W. Powell, *Thermal Conductivity, Nonmetallic Solids, Vol. 2, Thermophysical Properties of Matter* (IFI/Plenum, New York, 1970).
13. N. S. Saxena and I. Ul-Haq, *Int. J. Energy Research* **16**:489(1992).
14. S. Castellazi, M. R. Cimberele, C. Fredeghini, E. Giannini, G. Grasso, D. Marre, M. Putti, and A. S. Siri, *Physica C* **273**:314 (1997).
15. D. M. Ginsberg, *High Temperature Superconductivity* (World Scientific Publshing, London, 1992).
16. C. Uher, *J. Supercond.* **3**:337 (1990).